Study of calcium-silicate composite lightened by waste expanded perlite

P Sebestova[1], V Cerny[1] and R Drochytka[1]

[1] Brno University of Technology, Faculty of Civil Engineering, Veveri 331/95,602 00 Brno, Czech Republic

Email: sebestova.p@fce.vutbr.cz

Abstract. The term calcium-silicate composite can be recalled several basic building materials. The most common representatives are lime-silicate bricks and autoclaved aerated concrete. It is any material based on the reaction of lime and siliceous raw material. In this paper, attention is paid to composites based on autoclaved aerated concrete production technology. Possibilities of lightening the composite utilizing waste expanded perlite as a secondary raw material were investigated without the use of aluminium powder, which is commonly used in aerated concrete technology. Replacements of 10%, 30%, 50%, and 100% waste expanded perlite for sand were used. Based on physico-mechanical properties, and with the assessment of the microstructure, it has been found that up to 50% of the replacement of waste expanded perlite results in a lightening of the composite while increasing the compressive strength.

1. Introduction

The conventional substitution of quartz sand in autoclaved aerated concrete, whether partial or complete, if it would be possible to reduce the bulk density by substitution of sand with waste expanded perlite (WEP) and lightening of the composite without the use of aluminum powder.

As mentioned above, the calcium-silicate composite of interest is based on the autoclaved aerated concrete production technology. For clarity, this technology will be briefly described. The basic raw materials to produce autoclaved aerated concrete are lime, silica sand, and water. Cement, gypsum, and aluminium powder are also used. Lastly, other additives may be used, depending on the manufacturer. The raw materials are mixed to form a very fluid mixture to which aluminium powder is added at the end of the mixing. Then, the liquid mixture is poured into the mold. During the reaction of the aluminium powder with lime and water, hydrogen gas is produced, thereby aerating the liquid mixture. In this way, the porous concrete obtains its typical porous structure. After demolding and cutting the green body mass to the desired size, the intermediate is ready for curing. Curing performed in an autoclave at 180–190°C for 7–12 hours and at a pressure of 1.2–1.4 MPa (the temperature, time, and pressure of autoclaving vary by manufacturer). During curing, chemical reactions take place in the microstructure of the autoclaved aerated concrete, giving the resulting products their strength. After curing, the products are immediately ready for dispatch [1–3].

To understand the changes in microstructure, it is first necessary to describe the basic mechanisms of calcium hydro silicate (CSH) formation. The basic raw materials for the production of calcium-silicate composites are lime and quartz sand. These materials are characterized by oxide, they are primarily composed. Lime is a carrier of calcium oxide (CaO), silica sand contains a high amount of silica dioxides (SiO_2). The last important component for the formation of the CSH phase is water. However, the formation and interconnection of these three components would not have been so

Content from this work may be used under the terms of the Creative Commons Attribution 3.0 licence. Any further distribution of this work must maintain attribution to the author(s) and the title of the work, journal citation and DOI.
Published under licence by IOP Publishing Ltd

simple after mixing. The silica dioxides contained in the sand are in crystalline form, i.e. it is insoluble and under normal conditions, its reaction is very weak, and only on the grain surface. Therefore, it is necessary to cure the composites under hydrothermal conditions. During curing, SiO_2 reacts with CaO and H_2O to form a CSH phase. However, the CSH phases are many forms, and each form depends on the specific temperature, cure time, and ratio of individual oxides. For calcium-silicate composites, the CSH phase is an important 1.1 mm tobermorite. It is a layered mineral in the form of long needles, which connects individual grains of unreacted sand and ensures the strength of the product [4–7].

The effect of WEP on the calcium-silicate composite is a subject almost unexplored. Perlite is an amorphous volcanic rock that can be classified as a natural pozzolanic material due to its glassy structure, high silica dioxides, and alumina oxide content [8]. It is these two oxides, alumina oxide and silica dioxide, which are important for the use of WEP in the technology of autoclaved calcium-silicate composites. During perlite formation by the rapid cooling of ejected material in the water medium, about 5% of the water was bound to the rock, which is used in the production of expanded perlite. Perlite is heated to a temperature in the range of 900–1000°C, which converts the contained water into steam. As a result of the expansion of the material, expanded perlite is formed which has up to 4–20 times higher volume [8–11]. This also increases the specific surface area, so expanded perlite is a very porous material and thus becomes a good thermal insulator. WEP is characterized by low bulk density, fire resistance, and resistance to fungi and algae [9]. During the production of expanded perlite, WEP is formed, which belongs to the waste category "O" [12][13]. It can be further recycled, used as a secondary raw material, or deposit in construction waste dumps. Kotvica et al. [13] utilized ground expanded perlite as an additive to cement and increased compressive strength by up to 50% at 35% substitution. Further research has found that WEP is suitable for zeolite synthesis and suppresses the alkaline silica reaction when used in cement [13, 14]. In autoclaved aerated concrete, WEP was used as a substitute for quartz sand, and a 10% substitution resulted in a 15% reduction in thermal conductivity [1]. The possibility of using WEP is also confirmed by other studies dealing with the use of expanded perlite in autoclaved aerated concrete and fly ash-lime-gypsum mixture [15][16].

This experiment aimed to determine and define possibilities of lightening of autoclaved calcium-silicate composite with light filling. Waste expanded perlite (WEP) was chosen as a light filler. The data should then serve for further research into the use of lightweight filler in both calcium-silicate composite and autoclaved aerated concrete.

2. Materials and methods

2.1. Materials

Quartz sand, quicklime, cement, gypsum, and water were used to prepare the reference sample. Quartz sand (CZ, Dolní Lutyně) contains more than 92% silica dioxides. It can, therefore, be described as a very pure material. Quicklime (CZ, Beroun) is labeled CL 90-Q (R5, P1) according to ČSN EN 459-1 "Building quicklime". Portland cement has the designation CEM I 52.5 N (SK, Rohožník). Flue gas desulfurization (FGD) gypsum contains at least 95% calcium sulfate (CZ, Dětmarovice).

Table 1. Raw materials mixture.

Raw materials	REF [%]
Lime	9
Cement	14
FDG Gypsum	3
Quartz	75

Table 2. Chemical composition of raw materials.

Raw materials	Oxide	CaO	MgO	K_2O	Al_2O_3	P_2O	Fe_2O_3	MnO	Na_2O	SiO_2	TiO_2
WEP	[%]	1.26	0.23	4.56	13.10	0.02	2.02	0.06	2.14	74.00	0.16
Sand	[%]	0.23	0.16	1.53	2.53	0.01	0.84	0.01	0.70	92.91	0.14
Cement	[%]	64.25	2.02	3.32	5.40	0.16	3.06	0.10	0.36	19.67	0.31
Lime	[%]	95.62	0.79	-	-	-	-	-	-	-	-

The raw materials mixtures are based on the autoclaved aerated concrete technologies but without the use of aluminium powder (table 1). The chemical composition of raw materials is given in table 2.

Quartz sand was substituted by 10%, 30%, 50%, and 100% WEP in raw materials mixtures. The substitution was not in weight units, as is usual with other raw materials. Due to the very low bulk density of WEP, which was set at 300 kg/m^3, it was necessary to choose a substitution in volume units. The determined water-absorbing capacity of WEP was 260%. The chemical composition of WEP (CZ, Šenov u Nového Jičína) is given in table 2. The phase composition of WEP is quartz, cristobalite, muscovite, biotite, anorthite sodian, albite, and anorthoclase. The particle size distribution of WEP and quartz sand is given in Figure 1. Quartz sand contains the sand contains a higher proportion of fine grains. The curves have a similar increase. For this reason, the grain size distribution will be similar for WEP and quartz sand.

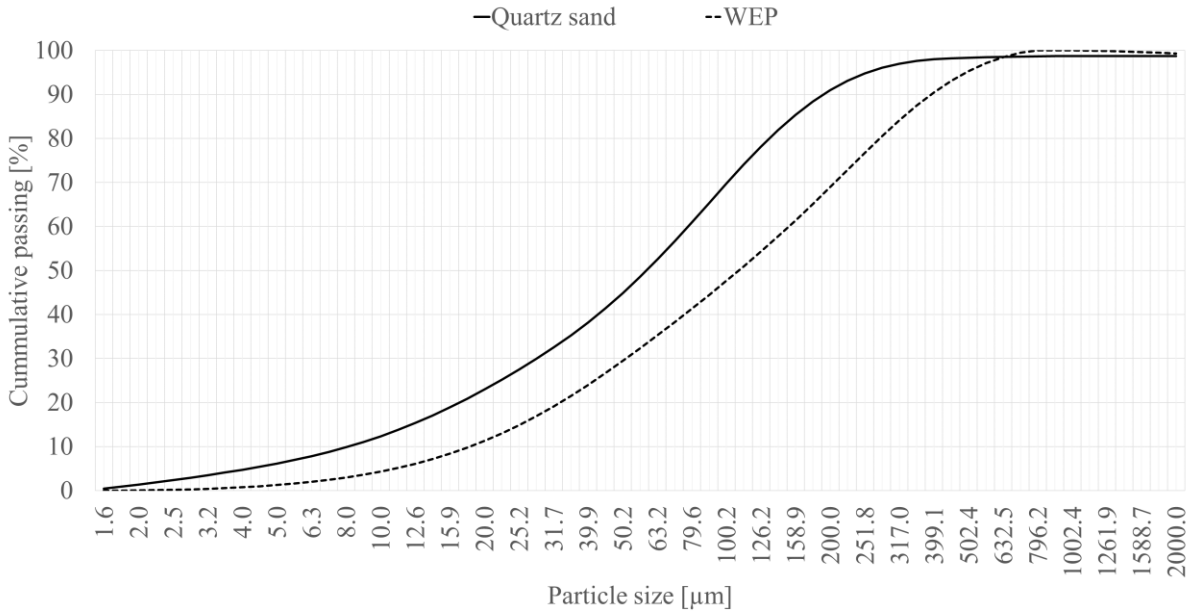

Figure 1. The grain size of WEP and quartz sand.

2.2. Preparation of mixture

The sand and gypsum were homogenized in a mixer separately. After careful mixing, water was added. Reactive components (lime, cement) and WEP were mixed into this mixture. the prepared liquid mixture was poured into molds of 40 × 40 × 160 mm. The flow test was immediately determined on the remaining mass. WEP is a very absorbent material. With such a high-water absorption, WEP can take up a large amount of water during mixing, which affects the resulting consistency of the mixture. To monitor the effect of the amount of WEP in the composition on its consistency, the water was constant.

After 24 hours maturing of the mixture in the molds, the samples were removed from the molds and placed in a laboratory autoclave. Curing was carried out at 190°C for 7 hours.

2.3. Methods

Basic physical-mechanical properties, such as compressive strength and bulk density according to ČSN EN 1351 and ČSN EN 678, were determined on the samples.

The microstructure of samples was studied by X-ray diffraction analysis and scanning electron microscope. The method of X-ray diffraction analysis is based on the fact that the crystal lattice of each mineral has a specific distance between two parallel surfaces. This value can be obtained at a known wavelength λ and a measured reflection angle θ. To be able to subject X-ray diffraction analysis, it was necessary to grind to a size of less than 20 μm in a so-called micromills. X-ray powder data were collected on an Empyrean PANalytical using Cu-cathode, $\lambda = 1.540598$ for Kα 1. Angular reproducibility is <0,0002°. For scanning by the electron microscope, it was again necessary to obtain central cores of samples, without contamination by surrounding impurities. These samples were then gold plated to ensure their conductivity. They were then inserted into the microscope body to remove residual moisture and air. Samples were analyzed on a TESCAN MIRA 3 XMU scanning electron microscope at an accelerating voltage of 20 kV.

The flow test is performed using a cylinder (height 5.4 cm, diameter 7.1 cm) and a plastic plate. The mixture is poured into the cylinder. The cylinder is raised and immediately after spilling the mixture, two perpendicular diameters are measured. The results are given in cm.

3. Results

3.1. Physical-mechanical properties

Figure 2 shows the physico-mechanical properties of samples with WEP substitution. The graph shows the dependence of compressive strength and flow of the mixture on bulk density. Each curve shows one dependence, namely the compressive strength on the bulk density and the flow of the mixture on the bulk density. The decrease in bulk density in the graph is dependent, inter alia, on the increasing amount of WEP substitution. The increasing WEP substitution value moves from right to left in the graph. The table with the values used is also shown in the graph.

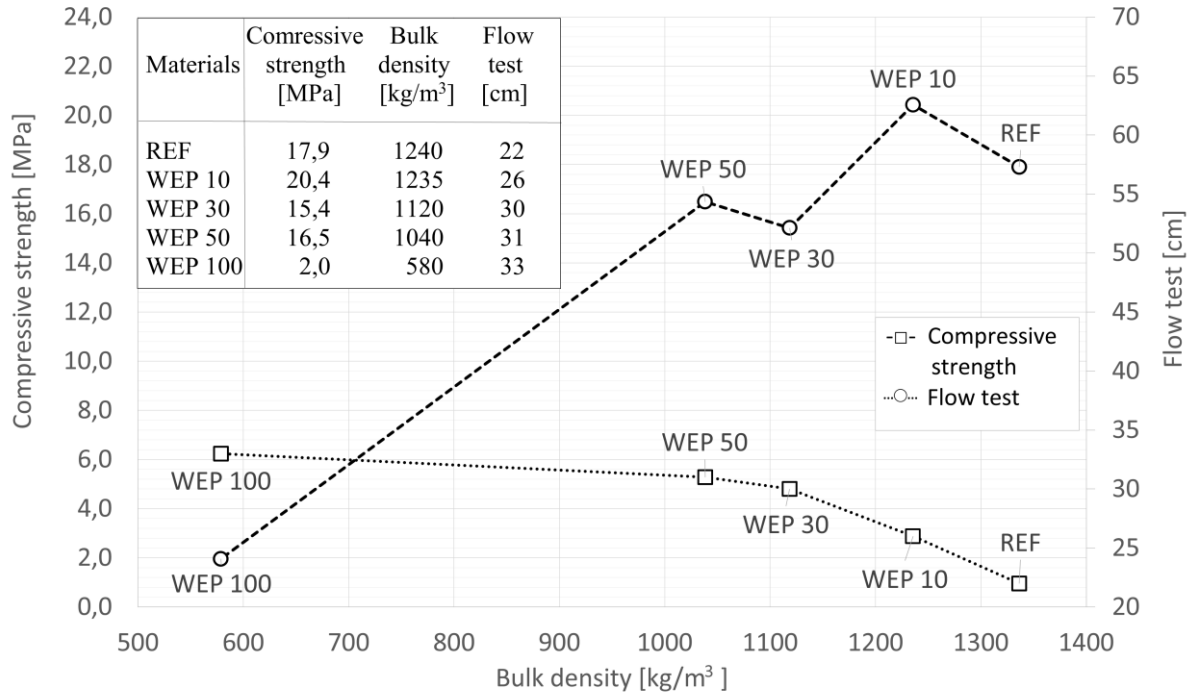

Figure 2. Physical-mechanical properties of calcium-silicate composite with substitution of WEP.

Interesting results were obtained when measuring the flow of the mixture. WEP has a high-water absorption capacity (260%) and it was expected that with higher sand substitution of WEP the flow of the mixture would decrease. However, the liquid mixture became more fluid. To elucidate the increase in the fluidity of the mixture, optical images if WEP were determined. In the images of WEP in water, an air layer formed around the WEP grain, which prevents water from penetrating its structure. The air layer disappears within a few minutes, creating only the apparent fluidity of the mixture. Therefore, a longer and more intensive mixing of the mixture is suggested.

One of the basic parameters of lightweight calcium-silicate composites is the bulk density. The calcium-silicate composite is characterized by a bulk density of 1450 kg/m^3. When WEP is used, the material is gradually lightened. Significant weight loss was recorded at 100% sand substitution by WEP.

The unexpected result was the achieved compressive strength of lightweight calcium-silicate composites. Up to 50% sand substitution, composites were lightened, and strength increased. At 100% sand substitution by WEP, the strength decreased to 0.6 MPa. However, considering the significant decrease in bulk density, the resulting calcium-silicate composite can be described as a potential thermal insulator.

3.2. Microstructure

As described in the introduction, it is necessary to identify newly formed minerals to explain the behavior of the properties of calcium-silicate composites. In this case, the focus is on the mineral 1.1 mm tobermorite, which is a carrier of strength. Images of the minerals are shown in Figure 4 and figure 4.

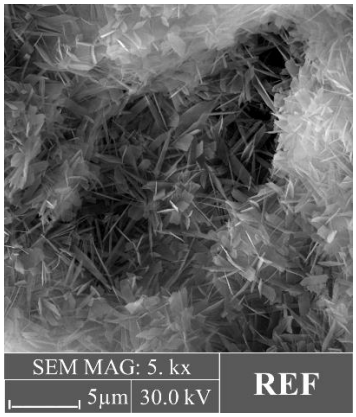

Figure 3. SEM images of the reference sample.

The calcium-silicate composite contains plate-like 1.1 mm tobermorite crystals. This shape of tobermorite is most often found in the crystalline quartz reaction. Tobermorite of composite with 10% sand substitution by WEP does not change its shape. In addition, a non-crystalline CSH gel is present in the sample. At 30% and 50% sand substitution by WEP, the shape „house of cards“ of 1.1 nm tobermorite described by Chucholowsky [17] occurs in his work. This shape of tobermorite is characterized by the support of compressive strengths, which has been manifested here. The composite with 100% substitution by WEP does not contain 1.1 nm tobermorite crystals. It contains long hairy new phases. These phases are called α-C_2SH and are formed as the first reaction product using 0.10–1 mm grain silicon sources [18].

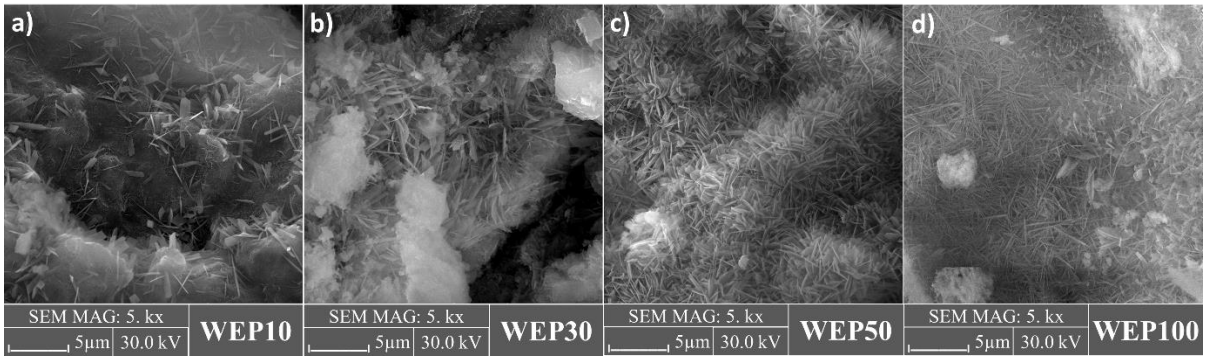

Figure 4. SEM images of calcium-silicate composite with sand substitution by WEP.

The microstructure of the composite can also be determined by X-ray diffraction analysis. In this analysis, it is possible to determine the degree of crystallization of the new phases using the intensity of the diffraction line. This analysis was also used in the research of expanded calcium-silicate composite. The hydrothermal conditions were adjusted such that the quartz surface was partially dissolved and released $H_3SiO_4^-$ or $H_2SiO_4^{2-}$ ions into the alkaline solution. These ions react with Ca^{2+} ions present in the alkaline solution to form crystalline calcium hydrogen silicate phases. For this reason, crystalline 1.1 mm tobermorite or other crystalline phases should appear in all samples. This assumption partly correlates with the results presented in Figure 5.

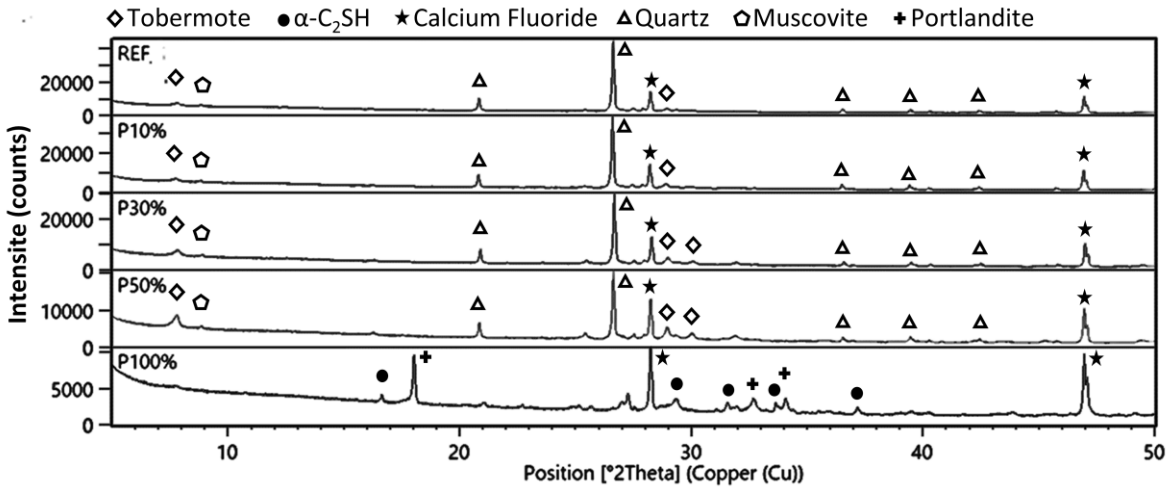

Figure 5. X-ray diffractograms of calcium-silicate composite with sand substitution by WEP.

Samples with the 10–50% sand substitution by WEP contain 1.1 mm tobermorite. In these samples, WEP increased the crystallization rate and the crystallization of tobermorite was most intense at 50% substitution. These samples also contain quartz and muscovite. These minerals are contained in the sand. Calcium Fluoride was added to the samples as standard.

1.1 mm tobermorite was not formed in the sample with 100% sand substitution by WEP. Quartz and muscovite are not present in the sample. Quartz and muscovite contain sand. Therefore, these minerals are not present in the sample with 100% sand substitution by WEP. However, there are other new phases in the sample. The sample contains α-C_2SH and portlandite. The results confirm the results of the SEM analysis.

4. Discussion

4.1. Structure formation used crystalline silica dioxides (sand)

In the case of the reference sample, which was formed using sand, that is, crystalline silica dioxides, it can be stated that this was a process of microstructure formation already described. As a result, a plate-like 1.1 mm tobermorite was formed which crystallized on the surface of the sand grains to form a solid bonding matrix between these grains. This is related to the achieved compressive strength, which is standard for a calcium-silicate composite.

4.2. Structure formation used crystalline silica dioxides (sand) and amorphous silica dioxides (WEP)

The combination of crystalline and amorphous silica dioxides, the formation of 1.1 mm tobermorite is inclined to the side of the higher amount of amorphous silica oxides. In previous studies [19][20], the positive effect of amorphous silica dioxides on the formation of 1.1 mm tobermorite was confirmed. The results obtained to confirm this statement. Another reason for the increased crystallization of tobermorite is in the porous character of WEP. The respective surface and hence the reaction surface of silicon sources makes a decisive role in the solubility behavior of silicon. Due to the high reaction surface, WEP dissolves to a greater extent and thus contributes to the crystallization of 1.1 mm tobermorite.

4.3. Structure formation used amorphous silica dioxides (WEP)

In the case of a sample with 100% sand substitution by WEP, unlike other samples, a crystalline 1.1 mm tobermorite was not formed. SEM and XRD analyses confirmed the presence of α-C_2SH, which is the primary curing product and is partially crystalline [18]. During later curing, α-C_2SH decomposes in favor of 1.1 mm tobermorite. However, in this sample, only the α-C_2SH, portlandite and CSH gel were formed which is evident in Figure 5. There may be several reasons why tobermorite is not formed.

The high curing temperature and reactivity of the silica dioxide cause the formation of a supersaturated solution. Increased dissolution changes the entry conditions for tobermorite formation. [21], [22] This phenomenon is also confirmed by the presence of portlandite. Portlandit is not involved in the reaction in its entirety, like other samples. Another explanation is in exceeding the curing temperature (180°C). The solubility curve according to states that the solubility curves of portlandite and amorphous silicon dioxides intersect at 120°C [22]. At higher temperatures, the solubility of portlandite decreases while the solubility of amorphous silica dioxides increases. As a result of this rule, the solution could be supersaturated in favor of silica dioxides. WEP is also characterized by porosity and thus generates a large reaction area which, in turn, may have resulted in a change in the entry ratio of calcium oxide to silica dioxides. According to studies, the ideal ratio for 1.1 mm tobermorite formation is 0.83, and an unstable calcium hydrogen silicate phase is formed at a higher ratio.

5. Conclusion

Nowadays, it is the duty to address sustainable technologies, environmental solutions, and efforts to recycle and use as much waste as possible. This study focused precisely on the use of waste material that waiting for its use. WEP is tested in the production of calcium-silicate composite. Research has shown that the recovery of this waste can have a positive effect on the properties of the composite. By using WEP, the compressive strength of composites was increased, and the bulk density of composites was reduced, too. At 100% sand substitution by WEP, a composite with a very low bulk density of 640 kg/m^3 and a compressive strength of 0.6 MPa was formed.

Acknowledgment

This paper was elaborated within project No. [FV30327] " Progressive high-quality autoclaved aerated concrete non-waste technology with usage of renewable resources", and was also funded under [FAST-J-20-6165] "Research of substitution of binder component of lime-silicate composites using alternative raw materials".

References

[1] Ling T, Mo K H, Qu L, Yang J and Guo L 2017 Mechanical strength and durability performance of autoclaved lime-saline soil brick *Const. Buil. Mat* **146** pp 403–409
[2] Dachowski R and Nowek M 2016 Landfill leachate as an additive in sand-lime products *Proc. Eng.* **161** p 572
[3] Pytel Z and Malolepszy J 2000 Effect of mineral admixtures on some properties of sand-lime bricks *Elsevier* pp 371–382
[4] Kurama H, Topcu İ B and Karakurt C 2009 Properties of the autoclaved aerated concrete produced from coal bottom ash *Jour. Mat. Proc. Tech.* **209** pp 767–773
[5] Zou J, Guo CH, Jiang Y, Wie C and Li F 2016 Structure, morphology and mechanism research on synthesizing xonotlite fiber from acid-extracting residues of coal fly ash and carbide slag *Mat. Chem. Phys.* **172** pp 121–128
[6] Mitsuda T 1982 Influence of starting materials on the hydrothermal reaction in the CaO-SiO_2-H_2O system *Jour. Jap. Assoc. Mineral.* **77** pp 317–329
[7] Rozycka A and Pichor W 2016 Effect of perlite waste addition on the properties of autoclaved aerated concrete *Constr. Buil. Mat.* **120** pp 65–71
[8] Kotwica Ł, Pichor W and Nocun-Wczezlik W 2016 Study of pozzolanic action of ground waste expanded perlite by means of thermal methods *Jour. Ther. Anal. Calor.* **123** pp 607–613
[9] Expandovaný perlit *Perlit.cz* (*Online* http://www.perlit.cz/expandovany-perlit/)
[10] Long W J, Tan X W, Xiao B X, Han N X and Xing F 2019 Effective use of ground waste expanded perlite as green supplementary cementitious material in eco-friendly alkali activated slag composites *Jour. Cl. Prod.* **213** pp 406–414
[11] Sengul O, Azizi S, Karaosmanoglu F and Tasdemir M A 2011 Effect of expanded perlite on the mechanical properties and thermal conductivity of lightweight concrete *Ener. Buil*

43 pp 671–676
[12] Expandovaný perlit: Bezpečnostní list *Perlit.cz* (*Online* http://www.perlit.cz/wp-content/uploads/2017/03/bezpecnosti-llist_EP.pdf)
[13] Kotwica Ł, PICHÓR W, Kapeluzsna E and Rozycka A 2017 Utilization of waste expanded perlite as new effective supplementary cementitious material *Jour. Cl. Prod.* **140** pp 1344–1352
[14] Singh M and Garg M 1991 Perlite-based building materials - a review of current applications *Const. Buil. Mat.* **5** pp 75–81
[15] Ayudhya B I N 2011 Compressive and splitting tensile strength of autoclaved aerated concrete containing perlite aggregate and polypropylene fiber subjected to high temperatures *Son. J. Sci. Technol.* **33** pp 555–563
[16] Demir I and Serhat Baspinar M 2008 Effect of silica fume and expanded perlite addition on the technical properties of the fly ash-lime-gypsum mixture Const. Buil. Mat. **22** pp 1299–1304
[17] Chucholowski C, Holger H and Thienel K 2018 Improving the recyclability, environmental compatibility, and CO_2 balance of autoclaved aerated concrete by replacing sulfate carrier and cement with calcined clays *Ce/papers* **2** pp 503–512
[18] Harmann A 2004 Untersuchungen zum Kristallisationsverhalten und zur Morphologie von 11 Å Tobermorit in Abhängigkeit von der Reaktivität der Kieselsäurequelle und dem Ionenbestand der Hydrothermallösung *Fach. Geowiss. Geog. Univer.* (Hanover)
[19] Ma B G, Cai L X, Jian S W and Su L 2014 Influence of Fly Ash Fineness on Autoclaved Energy Conservation Block's Performance and Hydration Products *Key Eng. Mat.* **599** pp 302–309
[20] Serhat Baspinar M, Demir I, Kahraman E and Gorhan G 2014 Utilization potential of fly ash together with silica fume in autoclaved aerated concrete production *KSCE Jour. Civil Eng.* **18** pp 47–52
[21] Dilmore R M and Nneufeld R D 2001 Autoclaved aerated concrete produced with low NO_x burner/selective catalytic reduction fly ash *Jour. Ener. Eng.* **127** pp 37–50
[22] Isu N, Teramura S, Ishida H and Mitsuda T 1995 Influence of quartz particle size on the chemical and mechanical properties of autoclaved aerated concrete (II) fracture toughness, strength and micropore *Cem. Noc. Res.* **25** pp 249–254
[23] Hartmann A, Pawlas G, Petrow V and Buhl J C 2014 Dissolution kinetics and phase transformations of autoclaved aerated concrete in alkaline and acid media without further additives *Jour. Sol. Waste Tech. Man.* **40** pp 97–109